




**Importance of kink energy in calculating the formation energy of a graphene edge**Wookhee Lee <sup>1</sup>, Daniel Hedman <sup>2</sup>, Jichen Dong,<sup>3</sup> Leining Zhang,<sup>4</sup> Zonghoon Lee,<sup>1,2</sup>  
Sung Youb Kim,<sup>1,5</sup> and Feng Ding <sup>2,6</sup><sup>1</sup>*Department of Materials Science and Engineering,**Ulsan National Institute of Science and Technology (UNIST), Ulsan 44919, Korea*<sup>2</sup>*Center for Multidimensional Carbon Materials (CMCM), Institute for Basic Science (IBS), Ulsan 44919, Korea*<sup>3</sup>*Beijing National Laboratory for Molecular Sciences Key Laboratory of Organic Solids Institute of Chemistry,  
Chinese Academy of Sciences, Beijing 100190, China*<sup>4</sup>*School of Chemistry and Chemical Engineering, Beijing Institute of Technology, Beijing 100081, China*<sup>5</sup>*Department of Mechanical Engineering, Ulsan National Institute of Science and Technology, Ulsan 44919, South Korea*<sup>6</sup>*Faculty of Materials Science and Engineering/Institute of Technology for Carbon Neutrality, Shenzhen Institute of Advanced Technology,  
Chinese Academy of Sciences, 1068 Xueyuan Blvd, Shenzhen 518055, China*

(Received 16 November 2022; accepted 17 May 2023; published 15 June 2023)

The formation energy of an arbitrary graphene edge or that of other 2D materials has been estimated as a summation of the armchair (AC) and zigzag (ZZ) edge sites. Such an estimation assumes that each site is independent from its neighboring sites, which is unlikely due to the overlap of electron densities. Here, we show that to accurately calculate the formation energy of graphene edges with various functional groups the energy of the junction between AC and ZZ sites, the “kink energy,” is essential. It is significant that the kink energies of graphene edges with different functional groups are all negative, namely, kink formation stabilizes the chiral graphene edges.

DOI: [10.1103/PhysRevB.107.245420](https://doi.org/10.1103/PhysRevB.107.245420)**I. INTRODUCTION**

Computational simulation in various fields, including physics, chemistry, astronomy, materials science, and biology, offers predictions of properties, behaviors, and processes in a physical and chemical manner. To obtain the desired level of accuracy in simulation results, the method of calculation must be chosen with care. It is well established that the highest level of accuracy can be achieved through quantum-mechanical calculation; however, the computational cost is constrained by the electronic degrees of freedom [1–5].

*Ab initio* molecular dynamics (AIMD) simulations differ from classical molecular dynamics (MD) [6–9] and Monte Carlo (MC) simulations [10–12] by using a quantum-mechanical approach to determine atomic forces from electronic structure calculations. While AIMD simulations provide a more accurate description of the electronic structure, they are limited to systems containing hundreds of atoms [13].

MD and MC simulations require the calculation of the system’s energy as a function of its configuration. The use of quantum-mechanical approximations and analytic potential-energy functions allows for the determination of the total energy and the force on each particle. However, the complexity of the system results in a wide range of analytic potential-energy functions.

One limitation of using analytic potential-energy functions is the difficulty in scaling to larger systems, due to the problem of transferability caused by model complexity. Additionally, models created for specific systems may be inaccurate for others. Therefore, proper analytic potential-energy functions with several adjustable fitting parameters are needed to model

various materials and qualitatively describe a range of phenomena.

There have been many simulation studies on 2D materials. Among the diverse 2D materials, graphene has many astounding characteristics which have drawn huge attention from researchers [14,15]. Especially the edges of graphene have an enormous diversity, which cause distinctive growth dynamics and unique electronic properties [16–19] similar to that of nanotubes [20,21].

One of the simplest models of graphene nanoribbons (GNRs) describes the formation energy of a graphene edge as a summation of the edge energies of all armchair (AC) and zigzag (ZZ) sites appearing at the edge [22]:

$$\gamma' = 2\gamma_{AC} \sin(\theta) + 2\gamma_{ZZ} \sin(30^\circ - \theta), \quad (1)$$

Here  $\gamma_{AC}$  and  $\gamma_{ZZ}$  denote the formation energy of an AC and ZZ site, respectively, and  $\theta$  is the chiral angle of the graphene edge. Such a simple model implies that each AC or ZZ site of a graphene edge is independent or the interactions between neighboring sites are negligible. Obviously, such an approximation is questionable because two neighboring sites and their functional groups have overlapping electron densities, such that the aromaticity of a graphene edge is configuration dependent, which means that altering the arrangement of the edge sites will change the stability of the edge or its formation energy [22–24]. The junction between AC and ZZ sites is generally ignored in most studies, such as the theoretical research on the edge stability of graphene [25–29] and other 2D materials including hexagonal boron nitrides (h-BN) [30–36], transition-metal

dichalcogenides [37–39], etc. [40–42], even though there are some exceptional studies [43–45].

There have been many attempts of modification on the edge of 2D materials for altering the characteristics of pristine characteristics. And, the functionalization with organic and inorganic molecules through the variety of covalent and non-covalent interactions is one of those modifications [46–53]. In addition, the edge formation energy varies in the presence of functionalization, especially at the edge sites [54–56]. There exists a diverse variety of functionalizations, such as hydrogenation, halogenation (-F, -Cl, -Br, and -I), sulfur (-S), thiol (-SH), and other functional groups i.e., methyl group (-CH<sub>3</sub>) or hydroxyl group (-OH). When the system is functionalized, out-of-plane distorted rippling occurs at the functionalized edges due to the relief the mechanism upon the structural deformation causes by the steric hindrance between two neighboring pairs of functional groups as the response of a 2D layered system to 1D edge strain [57–59]. The bonds formed between the carbon atoms and the terminated atoms such as H, F, and Cl indicates that there is a change in hybridization from  $sp^2$  to  $sp^3$  depending on the adsorption of termination atoms. This causes large alternations in the structural and electronic and magnetic properties of graphene edges or GNRs, such as the transition from semimetal to an insulator [48,60–62]. Hydrogenation and halogenation, which are simplest and the most manageable adsorption processes, are known to be one of the most efficient chemical modification strategies, resulting in numerous donors and acceptors [63].

In addition, fluorination is one of the renowned halogenations with strong bonding between carbon and fluorine atoms [64] and strong hybridization of the  $2p$  orbitals, which causes buckled structures with severe changes in bonding, significant distortion of the Dirac cone, and the absence of energy bands [65]. This applies to the other halogenations as well, for instance chlorination or methylation on account of the bonding between carbon and halogen atoms or functional groups [66].

In this study, we show that the kink energy contributes significantly to the stability of graphene edges, especially those with functional groups. Theoretical models that include the kink energy are essential for acquiring accurate results, such as the equilibrium shape of graphene flakes with the different functional groups. In conclusion, considering kink terms leads to the better understanding of the graphene edge.

## II. MODEL

Density-functional theory (DFT) calculations of formation energies for different graphene edges were conducted by using the Vienna *Ab initio* Simulation Package (VASP) with spin polarization [68–70]. The generalized gradient approximation parametrized by Perdew, Burke, and Ernzerhof was used as exchange-correlation potential [71]. The interaction between valence electrons was characterized by projector-augmented wave method [72,73] and the maximum energy cutoff for the plane waves was set to 400 eV. Graphene nanoribbons of different chiralities were used to model various graphene edges. The length of a GNR unit cell was on average 20 Å along the in-plane direction and the vacuum spacing associated with the out-of-plane direction was larger than 15 Å, to avoid the interaction between the periodic images. The

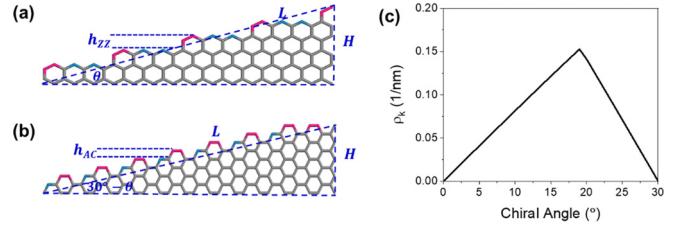


FIG. 1. Number of kinks on an arbitrary edge of graphene. (a) Kinks of a graphene edge near the zigzag direction ( $0^\circ < \theta < 19.107^\circ$ ), where  $h$  is the height of the kinks. (b) Kink formation of a graphene edge near armchair direction ( $19.107^\circ \leq \theta < 30^\circ$ ), where  $h$  is the height of the kinks. (c) Kink density as a function of the chiral angle of the edge.

Brillouin zone of models sampled at the  $\Gamma$  point and self-consistent field iterations were converged to a tolerance of  $10^{-4}$  eV. Relaxation of both atomic and lattice degrees of freedom was performed until the maximum force on all the atoms was smaller than  $0.01$  eV/Å.

The formation energy of a graphene edge can be obtained from DFT calculations as

$$E_\gamma = \frac{E - N_C \varepsilon_C - N_t \mu_t}{2L}, \quad (2)$$

where  $E$  is the DFT-calculated energy of the GNR.  $N_C$  and  $N_t$  are the numbers of carbon atoms and functional groups of the GNR, respectively.  $\varepsilon_C$  denotes the energy of a carbon atom in graphene,  $\mu_t$  is the chemical potential of the functional group, and  $L$  as the length of the GNR [54]. The kink energy of a graphene edge can then be calculated as follows:

$$\varepsilon_k = \frac{(2LE_\gamma - N_{ZZ}\varepsilon_{ZZ} - N_{AC}\varepsilon_{AC})}{N_k}, \quad (3)$$

In this expression,  $E_\gamma$  and  $L$  are the edge formation energy and the length of GNR, respectively.  $N_{ZZ}$  and  $N_{AC}$  denote the number of ZZ and AC, and  $N_k$  is the number of kink sites. The energy per AC and ZZ site is denoted by  $\varepsilon_{ZZ}$  and  $\varepsilon_{AC}$  and is obtained through the formation energy divided by the number of either AC or ZZ.

## III. RESULTS AND DISCUSSION

In general, the kink density is given as  $\rho_k = N_k/L$ , where  $N_k$  is the number of kinks for an edge of length  $L$ , where the largest kink density occurs at  $\theta = \tan^{-1} \frac{\sqrt{3}}{5} \approx 19.107^\circ$  [25,44]. The number of kinks for a straight edge of length  $L$  can be calculated as follows  $N_k = \frac{H}{h}$ , where  $H$  and  $h$  are the height of the two triangles formed by the edge and the step, respectively.  $H$  and  $h$  will vary depending on the chirality of the edge as shown in Fig. 1. For a graphene edge close to the zigzag direction ( $0^\circ < \theta < 19.107^\circ$ ) [Fig. 1(a)], the height of the step is  $h = \frac{3}{2}a$ , where  $a = 0.142$  nm is the C–C bond length in graphene and the height of the edge is  $H = L \sin \theta$ . For a graphene edge near armchair direction ( $19.107^\circ \leq \theta < 30^\circ$ ) [Fig. 1(b)], the kink height becomes smaller,  $h = \frac{\sqrt{3}}{2}a$ , and the height of the edge is  $H = L \sin(30^\circ - \theta)$ . Thus, the

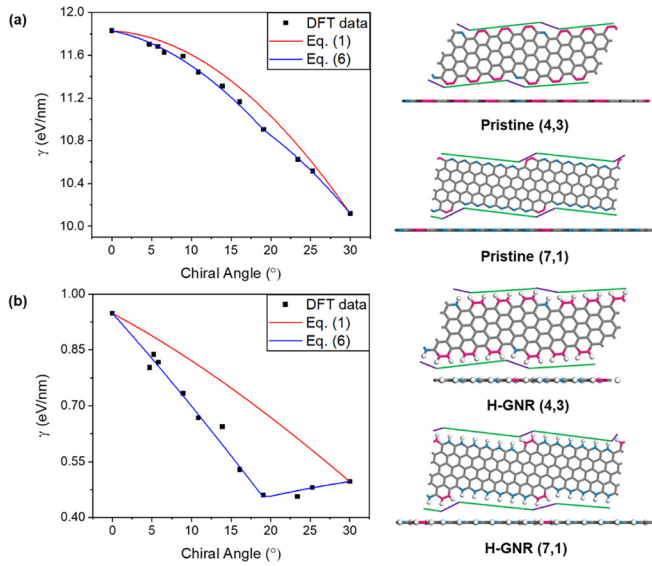


FIG. 2. Edge formation energy plots from DFT data, Eq. (1), and Eq. (5) and (4,3) (near AC) and (7,1) (near ZZ) structures of (a) pristine graphene nanoribbons and (b) hydrogenated graphene nanoribbons (H-GNRs). Magenta, and azure colors in models indicate armchair and zigzag sites, respectively. Hydrogen atoms are displayed as white balls and the green lines indicate the chiralities and the purple lines imply kink sites.

kink density for an edge of any chirality can be calculated as

$$\rho_k = \begin{cases} \frac{2 \sin(\theta)}{3a} & 0^\circ < \theta < 19.107^\circ \\ \frac{2 \sin(30^\circ - \theta)}{\sqrt{3}a} & 19.107^\circ \leq \theta < 30^\circ \end{cases} \quad (4)$$

Figure 1(c) shows the density of kinks of an arbitrary graphene edge, from which we can see that the edge along the direction of  $\theta = 19.107^\circ$  has the largest kink density. It is important to note that here we assume that the graphene edges are straight and thus all the kinks are single-height kinks.

By considering the contribution of kinks to the edge stability, the formation energy of a graphene edge, Eq. (1), can be rewritten as

$$\gamma = 2\gamma_{AC} \sin(\theta) + 2\gamma_{ZZ} \sin(30^\circ - \theta) + \rho_k \varepsilon_k, \quad (5)$$

where  $\rho_k$  is the kink density, which is calculated by Eq. (4) or (5), and  $\varepsilon_k$  is the kink energy from Eq. (3).  $\gamma_{AC}$  and  $\gamma_{ZZ}$  are the formation energy for an AC and ZZ edge, respectively, calculated using Eq. (2).

DFT-calculated edge formation energies,  $E_\gamma$ , of pristine, and hydrogen-terminated GNRs with different chiralities are shown in Fig. 2 together with the fitted models  $\gamma'$  and  $\gamma$ . Here, it is clear that the inclusion of the kink energy is important to accurately reproduce the DFT-calculated edge formation energies. For pristine graphene edges the simple model  $\gamma'$  has a maximum deviation from the DFT-calculated values of  $\sim 0.2$  eV/nm, a significant error, while the kink-energy corrected model  $\gamma$  fits the DFT data almost perfectly. The fitted kink energy  $\varepsilon_k = -0.1271$  eV per kink, which implies that the interaction between neighboring AC and ZZ sites lowers the energy; consequently, the simple model,  $\gamma$ , overestimates the formation energies of chiral edges as shown

TABLE I. Kink energy ( $\varepsilon_k$ ) used in the kink terms of Eq. (5), and edge formation energy of AC and ZZ in pristine-, H-, F-, and Cl-GNRs.

Types	$\varepsilon_k$ (meV)	$\gamma_{AC}$ (meV/Å)	$\gamma_{ZZ}$ (meV/Å)
Pristine GNRs	-127.1	1012	1183
H-GNRs	-150.0	49.66	94.84
F-GNRs	-141.3	594.4	528.5
Cl-GNRs	-143.4	596.0	586.7

previously [43]. Because of the very large formation energy of pristine graphene edges, the kink term contributes on average only 0.86% of the edge energy (see Supplemental Material, Table SI [67]) and the magnitude of the kink energy is only 5.6% of the difference in formation energy between AC and ZZ edges (see Supplemental Material, Table SI [67]).

For hydrogen-terminated graphene edges [Fig. 2(b)], the formation energy is much lower  $\sim 0.5$  to  $1.0$  eV/nm and the formation energy difference between AC and ZZ edges is only 0.5 eV/nm. However, the fitted kink energy ( $-0.15$  eV per kink) is close to that of the pristine edge, although slightly lower. Kink energies for other functional groups are shown in Table I, where it is clear that they are all similar to that of the hydrogen-terminated graphene edge. Comparing the two models for the hydrogen-terminated graphene edge shows that only with the kink energy can the model correctly predict the energy minima at  $\theta \approx 19^\circ$ ; the shapes

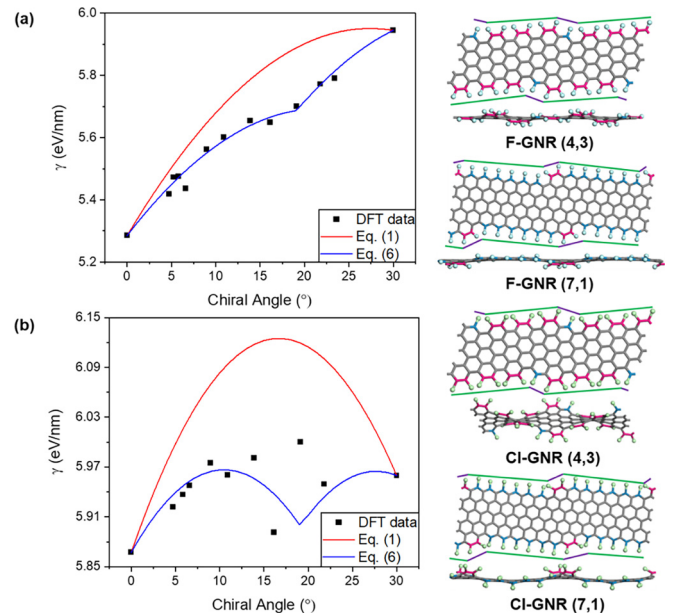


FIG. 3. Edge formation energy plots from DFT data, Eq. (1), and Eq. (5) and (4,3) (near AC) and (7,1) (near ZZ) structures: (a) rippled fluorinated graphene nanoribbons (F-GNRs) and (b) rippled chlorinated graphene nanoribbons (Cl-GNRs). Magenta and azure indicate armchair and zigzag sites, respectively. And, fluorine and chlorine atoms are displayed as cyan and mint balls, sequentially, and green lines indicate the chiralities and purple lines imply kink sites.


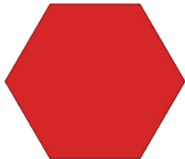
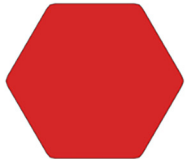


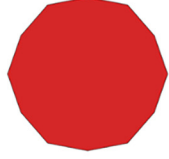

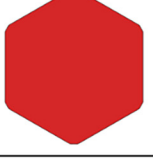
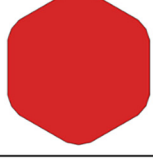
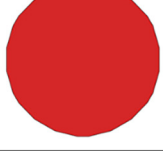
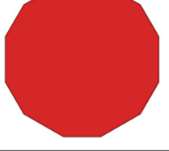
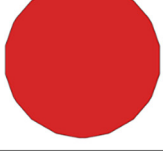
Types of GNRs	DFT	Old model: Eq. (1)	New model: Eq. (6)
pristine GNRs			
H-GNRs			
F-GNRs			
Cl-GNRs			

FIG. 4. Wulff constructions of the equilibrium shape of graphene based on DFT calculation results. Simple model [Eq. (1)], and including the kink term [Eq. (5)] of pristine-, H-, F-, and Cl- edges.

of the formation energy curves given by the two different models are also significantly different. This result clearly shows that a correct model of edge formation energy must include the kink energy; this is especially important for prediction of highly stable edges, which are also observed in experiments.

Figure 3 shows the formation energy of fluorinated and chlorinated graphene edges as function of edge chiral angle. For both cases, the model which includes the kink energy,  $\gamma$ , is significantly more accurate. The fitted kink energies are  $-0.1413$  and  $-0.1434$  eV per kink, respectively which are very close to that of hydrogenated graphene edge, while both the fluorinated and chlorinated graphene edges are rippled due to the repulsive interactions between the terminated atoms.

To demonstrate the importance of an accurate formation energy model, we calculated the equilibrium shapes of pristine graphene islands and those with different edge terminations (H-, F-, and Cl-) using Wulff construction theory [25,74]. The resulting equilibrium graphene shapes using the DFT data and fitted edge formation energies,  $\gamma$  and  $\gamma'$  are presented in Fig. 4. Here, it is clear that the kink energy is required to reproduce the proper equilibrium shapes of graphene. The equilibrium shapes predicated by Eq. (1) contain only AC or ZZ edges, which is a consequence of overestimating the formation energies of the tilted graphene edges. In contrast, including the kink term results in predicting the equilibrium shapes of graphene matching those of DFT, where tilted edges appear on the circumference of the graphene. The results of

Wulff construction clearly show the importance of the kink energy. And, the equilibrium shape of acquiring the Wulff construction through the polar plots and tangents is shown in Supplemental Material, Fig. S5 [67].

#### IV. CONCLUSION

In summary, through extensive density-functional theory calculations, we show that the energy of kinks appearing at the graphene edge is important. The energy of kinks on a graphene edge is negative, indicating that the tilted graphene edges could be more stable than AC or ZZ ones and, thus, is important to consider for applications. Besides the calculation of formation energies of graphene edges shown here, the kink energy will also play an important role in formation energies of other 2D materials, such as hexagonal boron nitride (h-BN), and transition-metal dichalcogenides.

#### ACKNOWLEDGMENTS

The authors acknowledge support from the Institute for Basic Science (Grants No. IBS-R019-D1 and No. IBS-R019-G1) and the support from Basic Research Laboratory (BRL) program (Grant No. 2021R1A4A1033224) of the National Research Foundation (NRF) of Korea, as well as the computation resources provided by the IBS high-performance computing cluster, the Simulator and Olaf.



- [1] A. J. Cohen, P. Mori-Sanchez, and W. Yang, *Chem. Rev.* **112**, 289 (2012).
- [2] C. J. Cramer, *Essentials of Computational Chemistry: Theories and Models*, 4th ed. (John Wiley & Sons, Inc., Chichester, West Sussex, 2004).
- [3] C. J. Cramer and D. G. Truhlar, *Phys. Chem. Chem. Phys.* **11**, 10757 (2009).
- [4] E. Apra, E. J. Bylaska, D. J. Dean, A. Fortunelli, F. Gao, P. S. Krstić, J. C. Wells, and T. L. Windus, *Comput. Mater. Sci.* **28**, 209 (2003).
- [5] F. Jensen, *Introduction to Computational Chemistry*, 3rd ed. (John Wiley & Sons, Inc., Chichester, West Sussex, 2017).
- [6] M. P. Allen and D. J. Tildesley, *Computer Simulation in Chemical Physics* (Springer Science & Business Media, Berlin, 2012).
- [7] Y. Dong, Q. Li, and A. Martini, *J. Vac. Sci. Technol. A* **31**, 030801 (2013).
- [8] J. A. Harrison, J. D. Schall, M. T. Knippenberg, G. Gao, and P. T. Mikulski, *J. Phys.: Condens. Matter* **20**, 354009 (2008).
- [9] M. O. Robbins and M. H. Müser, Computer simulations of friction, lubrication and wear, in *Modern Tribology Handbook*, edited by B. Bhushan (CRC Press, Boca Raton, Florida, 2001), pp. 717–765.
- [10] G. Raabe, in *Molecular Simulation Studies on Thermophysical Properties with Application to Working Fluids*, edited by E. Maginn (Springer Nature Singapore, Singapore, 2017), pp. 31–82.
- [11] R. Y. Rubinstein and D. P. Kroese, *Simulation and the Monte Carlo Method*, 3rd ed. (John Wiley & Sons, Inc., Hoboken, New Jersey, 2017).
- [12] J. M. Stubbs, *J. Supercrit. Fluids* **108**, 104 (2016).
- [13] E. Mosconi, J. M. Azpiroz, and F. De Angelis, *Chem. Mater.* **27**, 4885 (2015).
- [14] A. K. Geim, *Science* **324**, 1530 (2009).
- [15] M. S. Fuhrer, C. N. Lau, and A. H. MacDonald, *MRS Bull.* **35**, 289 (2010).
- [16] C. O. Girit, J. C. Meyer, R. Erni, M. D. Rossell, C. Kisielowski, L. Yang, C. H. Park, M. F. Crommie, M. L. Cohen, S. G. Louie, and A. Zettl, *Science* **323**, 1705 (2009).
- [17] C. K. Gan and D. J. Srolovitz, *Phys. Rev. B* **81**, 125445 (2010).
- [18] C. Hyun, J. Yun, W. J. Cho, C. W. Myung, J. Park, G. Lee, Z. Lee, K. Kim, and K. S. Kim, *ACS Nano* **9**, 4669 (2015).
- [19] X. Zhang, J. Xin, and F. Ding, *Nanoscale* **5**, 2556 (2013).
- [20] F. Ding, A. R. Harutyunyan, and B. I. Yakobson, *Proc. Natl. Acad. Sci. USA* **106**, 2506 (2009).
- [21] Y. Zhang, K. Cao, T. Saito, H. Kataura, H. Kuzmany, T. Pichler, U. Kaiser, G. Yang, and L. Shi, *Nano. Res.* **15**, 1709 (2022).
- [22] Y. Liu, A. Dobrinsky, and B. I. Yakobson, *Phys. Rev. Lett.* **105**, 235502 (2010).
- [23] K. Kim, S. Coh, M. F. Crommie, S. G. Louie, M. L. Cohen, and A. Zettl, *Nat. Commun.* **4**, 2723 (2013).
- [24] S. T. Skowron, I. V. Lebedeva, A. M. Popov, and E. Bichoutskaia, *Chem. Soc. Rev.* **44**, 3143 (2015).
- [25] V. I. Artyukhov, Y. Liu, and B. I. Yakobson, *Proc. Natl. Acad. Sci. USA* **109**, 15136 (2012).
- [26] R. Rao, D. Liptak, T. Cherukuri, B. I. Yakobson, and B. Maruyama, *Nat. Mater.* **11**, 213 (2012).
- [27] J. Dong, L. Zhang, B. W. Wu, F. Ding, and Y. Liu, *J. Phys. Chem. Lett.* **12**, 7942 (2021).
- [28] S. V. Erohin, L. A. Chernozatonskii, and P. B. Sorokin, *J. Phys. Chem. Lett.* **11**, 5871 (2020).
- [29] S. Feng, K. Cao, Y. Gao, Y. Han, Z. Liu, Y. Lu, and Z. Xu, *Commun. Mater.* **3**, 28 (2022).
- [30] A. Yamanaka and S. Okada, *Sci. Rep.* **6**, 30653 (2016).
- [31] J. A. Gonçalves, R. J. C. Batista, R. Tromer, and S. Azevedo, *Chem. Phys. Lett.* **727**, 126 (2019).
- [32] L. Ma and X. C. Zeng, *Nano Lett.* **17**, 3208 (2017).
- [33] Z. Zhang, Y. Liu, Y. Yang, and B. I. Yakobson, *Nano Lett.* **16**, 1398 (2016).
- [34] K. V. Bets, N. Gupta, and B. I. Yakobson, *Nano Lett.* **19**, 2027 (2019).
- [35] R. Zhao, J. Gao, Z. Liu, and F. Ding, *Nanoscale* **7**, 9723 (2015).
- [36] D. Li and F. Ding, *Mater. Today Adv.* **8**, 100079 (2020).
- [37] D. Davelou, G. Kopidakis, E. Kaxiras, and I. N. Remediakis, *Phys. Rev. B* **96**, 165436 (2017).
- [38] D. Cao, T. Shen, P. Liang, X. Chen, and H. Shu, *J. Phys. Chem. C* **119**, 4294 (2015).
- [39] N. Nayir, Y. Wang, Y. Ji, T. H. Choudhury, J. M. Redwing, L. Q. Chen, V. H. Crespi, and A. C. T. van Duin, *Mater. Sci. Eng.: B* **271**, 115263 (2021).
- [40] Z. Zhang, A. J. Mannix, X. Liu, Z. Hu, N. P. Guisinger, M. C. Hersam, and B. I. Yakobson, *Sci. Adv.* **5**, eaax0246 (2019).
- [41] K. V. Larionov, D. G. Kvashnin, and P. B. Sorokin, *J. Phys. Chem. C* **122**, 17389 (2018).
- [42] P. Hirvonen, V. Heinonen, H. Dong, Z. Fan, K. R. Elder, and T. Ala-Nissila, *Phys. Rev. B* **100**, 165412 (2019).
- [43] D. Hedman and J. A. Larsson, *SN Appl. Sci.* **2**, 367 (2020).
- [44] T. Ma, W. Ren, X. Zhang, and H. M. Cheng, *Proc. Natl. Acad. Sci. USA* **110**, 20386 (2013).
- [45] X. Kong, J. Zhuang, L. Zhu, and F. Ding, *npj Comput. Mater.* **7**, 14 (2021).
- [46] Q. H. Wang and M. C. Hersam, *Nat. Chem.* **1**, 206 (2009).
- [47] Y. Si and E. T. Samulski, *Nano Lett.* **8**, 1679 (2008).
- [48] A. Bostwick, T. Ohta, T. Seyller, K. Horn, and E. Rotenberg, *Nat. Phys.* **3**, 36 (2007).
- [49] T. Ohta, A. Bostwick, T. Seyller, K. Horn, and E. Rotenberg, *Science* **313**, 951 (2006).
- [50] D. C. Elias, R. R. Nair, T. M. G. Mohiuddin, S. V. Morozov, P. Blake, M. P. Halsall, A. C. Ferrari, D. W. Boukhvalov, M. I. Katsnelson, A. K. Geim, and K. S. Novoselov, *Science* **323**, 610 (2009).
- [51] X. R. Wang, X. L. Li, L. Zhang, Y. Yoon, P. K. Weber, H. L. Wang, J. Guo, and H. J. Dai, *Science* **324**, 768 (2009).
- [52] D. V. Kosynkin, A. L. Higginbotham, A. Sinitskii, J. R. Lomeda, A. Dimiev, B. K. Price, and J. M. Tour, *Nature (London)* **458**, 872 (2009).
- [53] K. P. Loh, Q. Bao, P. K. Ang, and J. J. Yang, *Mater. Chem.* **20**, 2277 (2010).
- [54] M. Vanin, J. Gath, K. S. Thygesen, and K. W. Jacobsen, *Phys. Rev. B* **82**, 195411 (2010).
- [55] E. Gracia-Espino, F. López-Urías, H. Terrones, and M. Terrones, *RSC Adv.* **6**, 21954 (2016).
- [56] P. Wagner, C. P. Ewels, J. J. Adjizian, L. Magaud, P. Pochet, S. Roche, A. Lopez-Bezanilla, V. V. Ivanoskaya, A. Yaya, M. Rayson, P. Briddon, and B. Humbert, *J. Phys. Chem. C* **117**, 26790 (2013).
- [57] P. Wagner, C. P. Ewels, V. V. Ivanoskaya, P. R. Briddon, A. Pateau, and B. Humbert, *Phys. Rev. B* **84**, 134110 (2011).

- [58] V. B. Shenoy, C. D. Reddy, A. Ramasubramaniam, and Y. W. Zhang, *Phys. Rev. Lett.* **101**, 245501 (2008).
- [59] E. Jomehzadeh and N. M. Pugno, *Compos. B: Eng.* **83**, 194 (2015).
- [60] G. Lee and K. Cho, *Phys. Rev. B* **79**, 165440 (2009).
- [61] Z. Ding, J. Jiang, H. Xing, H. Shu, R. Dong, X. Chen, and W. J. Lu, *Comput. Chem.* **32**, 737 (2011).
- [62] M. J. Park, J. K. Lee, B. S. Lee, Y. W. Lee, I. S. Choi, and S. Lee, *Chem Mater.* **18**, 1546 (2006).
- [63] K. E. Whitener, Jr., *J. Vac. Sci. Technol. A* **36**, 05G401 (2018).
- [64] S. O. Olanrele, Z. Lian, and C. Si, *RSC Adv.* **9**, 37507 (2019).
- [65] N. T. T. Tran, D. K. Nguyen, O. E. Glukhova, and M. F. Lin, *Sci. Rep.* **7**, 17858 (2017).
- [66] V. Georgakilas, M. Otyepka, A. B. Bourlinos, V. Chandra, N. Kim, K. C. Kemp, P. Hobza, R. Zboril, and K. S. Kim, *Chem. Rev.* **112**, 6156 (2012).
- [67] See Supplemental Material at <http://link.aps.org/supplemental/10.1103/PhysRevB.107.245420> for the different GNRs to calculate edge formation energy of Figs. 2 and 3; additional data of methylated GNRs; the whole process of equilibrium shapes of various GNRs shown in the main text; the contribution of kink terms on the energetics; the length and the number of AC, ZZ, kink, carbon in graphene, and termination groups; and even the formation energy of AC, and ZZ, and the edge formation energy difference from maximum and minimum values of diverse GNRs.
- [68] G. Kresse and J. Hafner, *Phys. Rev. B* **48**, 13115 (1993).
- [69] G. Kresse and J. Furthmüller, *Comput. Mater. Sci.* **6**, 15 (1996).
- [70] J. Robles and L. J. Bartolotti, *J. Am. Chem. Soc.* **106**, 3723 (1984).
- [71] J. P. Perdew, K. Burke, and M. Ernzerhof, *Phys. Rev. Lett.* **77**, 3865 (1996).
- [72] P. E. Blöchl, *Phys. Rev. B* **50**, 17953 (1994).
- [73] G. Kresse and D. Joubert, *Phys. Rev. B* **59**, 1758 (1999).
- [74] P. S. Branicio, M. H. Jhon, C. K. Gan, and D. J. Srolovitz, *Model. Simul. Mater. Sci. Eng.* **19**, 054002 (2011).